Observation of neutronless fusion reactions in picosecond laser plasmas

V. S. Belyaev, A. P. Matafonov, and V. I. Vinogradov
Central Research Institute of Machine Building, Korolev, Moscow Region, Russia

V. P. Krainov
Moscow Institute of Physics and Technology, 141700 Dolgoprudny, Moscow Region, Russia

V. S. Lisitsa
Institute of Nuclear Fusion, RSC "Kurchatov Institute," 123182 Moscow, Russia

A. S. Roussetski
P.N. Lebedev Physical Institute, Russian Academy of Sciences, 117333 Moscow, Russia

G. N. Ignatyev and V. P. Andrianov
Research Institute of Pulse Technology, Moscow, Russia
(Received 22 March 2005; revised manuscript received 6 May 2005; published 10 August 2005)

The yield of α particles in neutronless fusion reactions $^{11}B+p$ in plasmas produced by picosecond laser pulses with the peak intensity of 2×10^{18} W/cm^2 has been observed. Experiments were carried out on the "Neodymium" laser facility at the pulse energy of 10–12 J and pulse duration of 1.5 ps. The composite targets $^{11}B+(CH_2)_n$ were used. The yield of 10^3 α particles per pulse has been observed. The energy spectrum of α particles contains two maxima: at 3–4 MeV and at 6–10 MeV. The first of these peaks corresponds to the secondary α_{12} particles at the decay of the intermediate first excited state of ^{8}Be, whereas the second peak demonstrates generation of α_1 particles in the reaction $^{11}B+p$ with the production of this excited state. Simultaneous measurements of neutrons result in zero yield, which proves the observation of neutronless fusion reactions in our experiments.

DOI: 10.1103/PhysRevE.72.026406 PACS number(s): 52.58.Ei, 41.75.Jv, 52.50.Jm, 52.38.Ph

The investigation of neutronless fusion reactions in plasmas presents an important problem with respect to peaceful applications of nuclear energy. The analysis of these reactions for systems with magnetic confinement requires very difficult conditions upon plasma parameters because of high values of ionic temperature, which are needed for initiation of these nuclear reactions. Oppositely, high kinetic energies of atomic ions can simply be obtained in plasmas produced by intense ultrashort laser pulses. Therefore, it is interesting to directly check the generation of neutronless fusion reaction in plasmas produced by ultrashort laser pulses.

In this paper we present results of experiments in which the initiation of the neutronless fusion reaction $^{11}B+p$ has been observed in picosecond laser plasmas. These results were obtained on the 10 TW laser facility "Neodymium" [1] (Korolev City, Moscow Region, Russia).

The laser setup has the following parameters: pulse energy up to 15 J, wavelength of 1.055 μm, and pulse duration of 1.5 ps. The laser radiation is characterized by the presence of three prepulses. Two prepulses of picosecond duration at 13 ns and 25 ps, respectively, appear before a main laser pulse. They have a relative intensity of 10^{-4} and 10^{-3} with respect to the main pulse. The third prepulse is produced by the amplified spontaneous emission; it has the duration of $\sim$4 ns and relative intensity of 10^{-8} with respect to the main pulse. The focusing system provides a concentration of 40% of laser energy into the spot with of 15 μm diam; the peak laser intensity on the target surface is 2×10^{18} W/cm^2.

The experimental device is presented in Fig. 1. The laser beam is focused by the off-axis parabolic mirror with the focusing length of 20 cm into the solid target T at an angle of 40 deg to normal of the target.

The composite targets $^{11}B+(CH_2)_n$ with a thickness of 300 and 500 μm and containing 50% (weight) of ^{11}B atoms were studied in our experiments. Targets from the polyethyl-

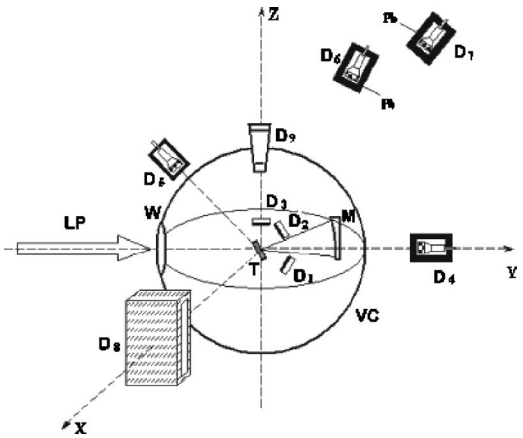

FIG. 1. A schematic of the experimental laser setup is shown. The various aspects are as follows: T, target; M, off-axis parabolic mirror; W, the window of the vacuum chamber, LB, laser beam; VC, vacuum chamber; D1–D3, track detectors CR-39; D4–D7, scintillation detectors of γ radiation; D8, detector of neutrons on helium counters; and D9, obscure chamber with the recording matrix.

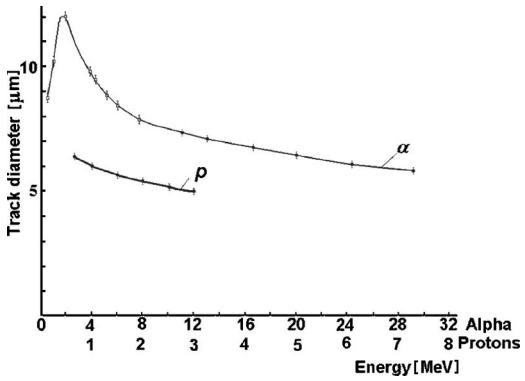

FIG. 2. Dependences of track diameters of protons and α particles on their energy.

ene $(CH_2)_n$ with a thickness of 400 μm were used for control experiments. Track detectors CR-39 covered by aluminum foil with a thickness of 6, 11, and 22 μm were applied for registration of α particles produced in the nuclear reaction

$$p + {}^{11}\mathrm{B} \rightarrow 3{}^{4}\mathrm{He} + 8.7\ \mathrm{MeV}. \quad (1)$$

Detectors were placed in a vacuum chamber at various angles (0,45,85 deg) to the normal of the target and at various distances from target (1.8 and 2.4 cm). The pressure of the rest gas was $<10^{-3}$ Torr. Using of detectors with different covers allows one to determine the type of particles, whereas measurements at various angles allow one to estimate their angular distribution.

The calibration of detectors CR-39 has been made using proton beams from a Van de Graaf accelerator (E_p=0.75–3.0 MeV) and also using standard α sources (E_α=0.4–7.7 MeV) and cyclotron α sources (E_α =8–30 MeV) of the Institute of Nuclear Physics of Moscow State University. Detectors were etched after irradiation during 7 h in a solution of NaOH in H_2O at 70 °C; then they were investigated in microscope MBI-9. Results of calibration, i.e., dependences of track diameters of protons and α particles on their energy, are presented in Fig. 2.

Preliminary measurements and our previous theoretical estimates [2] have shown that in the nuclear reaction, Eq. (1), other groups of α particles having energies of 6–10 MeV should be observed, besides α particles with an average energy of 2.9 MeV. These α particles are determined by the state of the intermediate nucleus ^{8}Be.

In this experiment we chose tracks of α particles among the background of tracks of other atomic ions ejected from the target during the laser pulse. The following experimental method was used. According to the calibration data (see Fig. 2) α particles with energies of 2–8 MeV have tracks with the diameters of 7.8–12 μm; an effect can be observed for these track diameters. This range was divided into two ranges: 7.8–10 μm and 10.2–12.0 μm. The estimate of α particle yields is based on subtraction of track densities for the $^{11}\mathrm{B}+(CH_2)_n$ target and pure $(CH_2)_n$ target. Then this quantity was multiplied by the efficiency of measurements, which is determined by the geometric factor (i.e., by the distance between the detector and target).

The scintillation plastic and stilbene detectors had been used for observation of hard x-rays. They were placed at a distance of 20 cm–4 m from the target. Pb filters with a thickness of 2–13.5 cm were placed before detectors. The detector of neutrons containing helium counters had been used for observation of neutron emission. It was placed on 18 cm from the target. The detector dimensions are the next: the width is 45 cm, height is 20 cm, and thickness is 10 cm. The side surfaces of the detector are covered by polyethylene $(CH_2)_n$ having a thickness of 2 cm. Neutrons produced by the short (1.5 ps) laser pulse were delayed in the plastic up to the thermal energy; respectively, they were registered by helium counters during different times. Thus, the registration time for neutron yield is increased. The efficiency of the neutron registration from the stationary neutron source of ^{252}Cf was about of 50%. The obscure camera with the recording matrix was used for control of the spot focusing diameter and for an estimate of the intensity of the x-ray in the range of 1–5 keV.

Two types of experiments were carried out. First, detectors CR-39 were exposured after a single irradiation of the target; then these detectors were exposured after multiple irradiation.

Results of measurements show that the effect does not exceed the background in the case of detectors covered by 6 μm Al. The background is produced by the penetration of strange ions through the filter. Their tracks can have diameters of the same size as that for the investigated α particles. Using detectors covered by 11 μm Al, we observed an excess of the effect over the background in both ranges of track diameters of α particles.

Estimations of the yield of α particles for detectors covered by 11 and 22 μm Al are given in Table I. The maximum effect was observed for diameters of 7.8–10 μm (the ratio of effect and/or background is equal to 4–11 for various detectors). The maximum efficiency of α-particle emission was measured for detectors that were placed at angles of 0 and 45 deg to normal of the target. The decreasing α-particle yield for the detector that was placed at an angle of 85 deg can be explained by the fact that a large amount of matter occurs on the tracks of α particles. The average yield of α particles into 4π solid angles for this range of track diameters is estimated as $\langle N_\alpha \rangle = 1.77 \times 10^3$. Some effects (the ratio of effect and/or background is equal to 2) are observed also for track diameters of 10.2–12.0 μm. In this case, the average yield of α particles is $\langle N_\alpha \rangle = 1.2 \times 10^3$.

At multiple irradiation, the average yields of α particles per one burst for detectors covered by 11 μm Al, are equal to 1.5×10^3 and 2.3×10^3 for track diameters in the ranges 7.8–10 and 10.2–12 μm, respectively (into the solid angle 4π Sr). For detectors covered by 22 μm Al, these yields are equal to 2.3×10^2 and 3×10^2, respectively.

The resulting distribution of track diameters based on measurements of six pairs of detectors covered by the Al foil with the thickness of 11 μm is shown in Fig. 3. Peaks with d=7.8–8.6 μm ($E_\alpha \sim$ 6–8 or 0.3–0.4 MeV) and with d=9.8–10.0 μm ($E_\alpha \sim$ 4 or 0.8 MeV) are observed. The broad maximum is observed also for d=10.8–12 μm ($E_\alpha \sim$ 1–3 MeV). These peaks demonstrate the possibility

TABLE I. Estimates of α particle yields in the Eq. (1) reaction.

Detector position	No. of bursts	Detector covering	n_α (7.8–10 μm)	n_α (10.2–12.0 μm)
R (cm)/φ deg		(μm Al)	(in 4π Sr)	(in 4π Sr)
1.8/85	1	11	1.6×10^3	[a]
2.4/0	1	11	1.8×10^3	10^3
2.4/45	1	11	1.9×10^3	1.4×10^3
1.8/85	3	11	1.1×10^3	8×10^2
2.4/0	3	11	2.4×10^3	[a]
2.4/45	3	11	10^4	2×10^4
1.8/85	2	22	5×10^2	1.6×10^3
2.4/0	2	22	3×10^2	1.4×10^3
1.8/85	2	22	5.5×10^2	[a]

[a]Effect does not exceed the background.

for emission of monoenergetic α particles with the kinetic energy of $E_\alpha > 3$ MeV, which are produced in the reaction $^{11}B+p$ via different states of the intermediate nucleus ^{8}Be.

More exact measurements of the α-particle energy were carried out taking into account the data for detectors covered by 22 μm Al (see the distribution in Fig. 4). Only one small maximum occurs at $d=7.8$ μm ($E_\alpha \sim 7.5$ MeV). The initial energy of α particles, which takes into account the energy losses in 22 μm Al, can be estimated as $E_\alpha \sim 10$ MeV. Some excess above the background is also observed at $d=10-11$ μm ($E_\alpha \sim 2.5-3$ MeV). The initial energy of α particles in this case is equal to 5.5–5.7 MeV. Disappearance of maxima that were observed in Fig. 3 demonstrates that they correspond to α particles with energies of 3–5 MeV.

Thus, the conclusion can be made that α particles with initial kinetic energies about of 3.4 ± 0.4, 4.0 ± 0.4, 5.6 ± 0.3, and 10 ± 1 MeV were observed in our experiments. The main part of the radiated α particles (up to 90%) have energy of <5 MeV.

Measurements using the obscure camera demonstrate that the diameter of the focusing spot for the soft x-ray range of 1–5 keV is of the order of 15 μm; this is in agreement with the measurements of the focusing spot at the laser wavelength of $\lambda=1.055$ μm.

It follows from our experiments that the photon energy of x-rays at a laser intensity of $\sim10^{17}$ W/cm^2 is concentrated in the range of several kiloelectron volts. However, a sharp increase of the number of hard x-ray photons with the energy of some megaelectron volts occurs when the laser intensity increases up to 2×10^{18} W/cm^2. It is important that the number of soft x-rays does not change. The conclusion can be made that a significant part of laser energy is transformed to the energy of fast electrons at superstrong laser intensities.

The detector using helium counters did not show registration of the neutron emission in these experiments. Indeed, it is seen from Fig. 5(a) that oscillograms of a neutron detector contain only one peak; it is produced at the irradiation of the detector by γ radiation of laser plasma and by the noise of laser setup. In Fig. 5(b) oscillograms of the same neutron detector are shown; they were obtained by means of measurement of the neutron yield from laser plasma for the target from deuterated polyethylene $(CD_2)_n$ with a thickness of 350 μm at the same laser intensity. The neutron yield is observed during 400 μs, which corresponds to the calculated lifetime of neutrons in this detector. The neutron yield measured by an activation detector is equal to 10^6 in 4π Sr per one laser pulse.

The energy distribution of α particles is characterized by two energy ranges: 3–4 and 6–10 MeV. The first range cor-

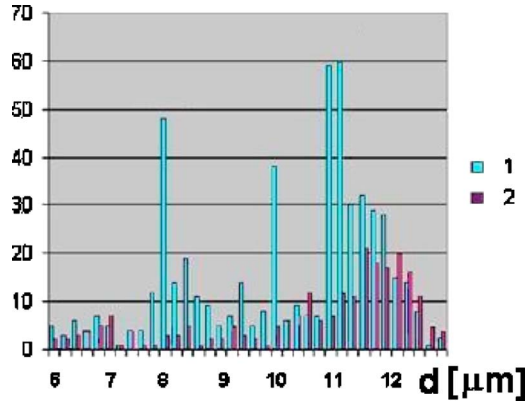

FIG. 3. (Color online) Total distributions of track diameters (number of tracks) for detectors covered with 11 μm Al. The detector area is 3 cm^2: 1, target $^{11}B+(CH_2)_n$ and 2, target $(CH_2)_n$.

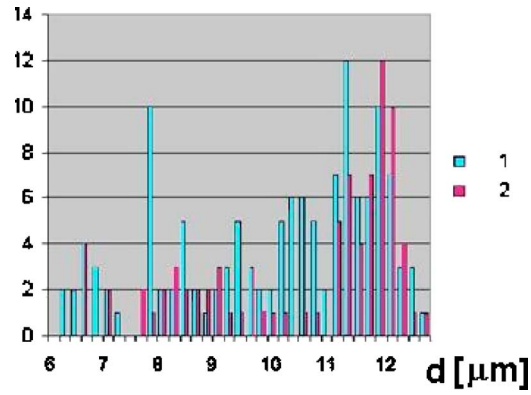

FIG. 4. (Color online) The same as in Fig. 3, but with 22 μm Al. The detector area is 1.5 cm^2: 1, target $^{11}B+(CH_2)_n$ and 2, target $(CH_2)_n$.

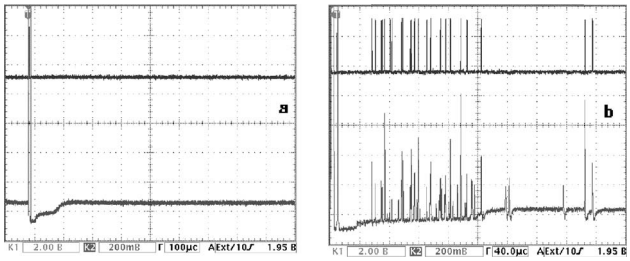

FIG. 5. Oscillograph records from neutron detector D8 using helium counters (the upper part presents digital data of detector, the lower part presents analog data): (a) the target is the composite material $^{11}B+(CH_2)_n$ with a thickness of 500 μm, (b) the target is the deuterated polyethylene $(CD_2)_n$ with a thickness of 350 μm.

responds to the production of α_{12} particles in the reactions [3–5]

$$^{11}B + p \rightarrow \alpha_0 + {}^{8}Be + 8.586 \text{ MeV},$$

$$^{11}B + p \rightarrow \alpha_1 + {}^{8}Be^{*} + 5.65 \text{ MeV},$$

$$^{8}Be^{*} \rightarrow \alpha_{12} + \alpha_{12} + 3.028 \text{ MeV}.$$

The secondary α_{12} particles are produced at the decay of the excited nucleus $^{8}Be^{*}$. This main channel has a sharp peak at the proton energy of 163 keV and a broad maximum at the proton energy of 660 keV. Kinematics of this reaction results in generation of α_{12} particles with the energies of 2–4 MeV. These α_{12} particles acquire the additional kinetic energy from the kinetic energies of protons and boron ions. The probability for the production of α_0 particles and of the ground-state ^{8}Be is very small [4]. A small number of the observed 10 MeV α particles can be attributed to this channel. The increase of α-particle energy also takes place from a small number of high-energy protons and boron ions in the tail of their energy spectra.

The second range corresponds, in our opinion, to the α_1 particles in the second channel. These α_1 particles also acquire the additional kinetic energy from the kinetic energies of colliding protons and boron ions.

Most α particles are produced in an overdense part of laser plasma, which has a depth on the order of skin-layer depth (i.e., <0.1 μm). Estimated losses of the α-particle energy do not exceed 10 keV. Therefore, the stopping range of α particles in this part of the plasma can be neglected. The stopping range of α particles in the underdense part of plasma can be neglected because of its low density. Thus, the observed energy spectrum of α particles is not distorted by their stopping in the target. Another effect is the charging of the target. The electrostatic potential of the target can both accelerate and decelerate the ejected α particles. The role of this effect is unclear. We estimate that the variation of the energy does not exceed 100 keV, while the kinetic energy of the α particle is equal to several megaelectron volts.

Thus, the obtained results demonstrate the possibility of neutronless nuclear reactions in plasma of picosecond laser pulses. This is explained by the high kinetic energy of atomic ions in laser plasma. The mechanism of the acceleration of protons and boron ions in the laser field is a subject for further consideration. The most probable mechanism is the charge separation after the fast axial ponderomotive repulsion of electrons from the laser spot to the periphery. It produces the axial quasistationary electric field which accelerates protons and atomic ions [6–9]. In the case of thin foils and superintense laser pulses, high-energy heavy ions are accelerated mainly on the rear side, away from the target [10], where their potential for nuclear interaction is negligible. In our case all nuclear reactions occurs in the thin dense-skin layer on the front surface of the relatively thick target.

The $p+^{11}B$ fusion rate coefficient is sufficiently high, even in the low-energy part of the proton spectrum. In the range of 100–300 keV proton energy the value of $\langle \sigma v \rangle$ increases from 1×10^{-16} to 3×10^{-16} cm^3/s [3]. This results in high efficiency of the fusion reaction (see also detailed derivations of α-particle yield in [2]).

Direct measurements of ion energies in laser plasmas were carried out in our other experiments at the peak laser intensity of $\sim10^{18}$ W/cm^2; they are based on the measurements of Doppler spectrum of the hydrogenlike F ions [11]. Results of these measurements demonstrate the generation of fast F ions with energies exceeding 1 MeV. The yield of protons with energies of 100–200 keV was observed in Ref. [12] at the peak laser intensity of 10^{18} W/cm^2. These data are in good agreement with the experimental data of Ref. [13] as well as with numerical simulations in the same paper. Experiments [8] at much higher intensities of 10^{19}–10^{20} W/cm^2 demonstrate acceleration of multicharged atomic ions. The ion energies exceed tens and hundreds of megaelectron volts; the energy spectrum of protons has cut off at 10 MeV. Thus, the generation of α particles with the above-cited values of kinetic energy measured in our experiments is in qualitative agreement with the observed spectra of protons and heavy atomic ions.

In conclusion, the possibility of initiation of neutronsless fusion reaction in plasma of picosecond laser pulses has been demonstrated. The yield of the order of 10^3 α particles in 4π Sr per one laser pulse in the fusion reaction $^{11}B+p$ has been measured at the peak laser intensity of 2×10^{18} W/cm^2. Simultaneous measurements of neutrons result in zero yield, which proves the observation of neutronless fusion reactions in our experiments.

ACKNOWLEDGMENTS

This work was supported by the International Science and Technology Center (Project No. 2155), by RFBR (Project No. 05-02-16551), and partially by INTAS (Project No. 03-54638). Authors thank F. E. Chukreev and D. Hoffmann for useful discussions.

[1] V. S. Belyaev, A. P. Matafonov, G. N. Ignat'ev, V. P. Andrianov, and A. Ya. Faenov, in *Proc. of 31st EPS Conference on Plasma Physics and Controlled Fusion*, London, 28 June–2 July 2004 ECA, Vol. 28G, p. 2.039 (2004).
[2] V. P. Krainov, Laser Phys. Lett. **2**, 89 (2005).
[3] W. M. Nevins and R. Swain, Nucl. Fusion **40**, 865 (2000).
[4] H. W. Becker *et al.*, Z. Phys. A **327**, 341 (1987).
[5] J. Liu *et al.*, Nucl. Instrum. Methods Phys. Res. B **190**, 107 (2002).
[6] S. C. Wilks *et al.*, Phys. Plasmas **8**, 542 (2001).
[7] K. Krushelnick *et al.*, Phys. Plasmas **7**, 2055 (2000).
[8] E. L. Clark *et al.*, Phys. Rev. Lett. **85**, 1654 (2000).
[9] I. Spencer *et al.*, Phys. Rev. E **67**, 046402 (2003).
[10] J. Fuchs *et al.*, Phys. Rev. Lett. **94**, 045004 (2005).
[11] V. S. Belyaev, A. Ya. Faenov, A. P. Matafonov, T. A. Pikuz *et al.*, Abstract of 32st EPS Conference on Plasma Physics and Controlled Fusion, Tarragona, Spain, 2005 (unpublished).
[12] S. Okihara *et al.*, Phys. Rev. E **69**, 026401 (2004).
[13] H. Habara *et al.*, Phys. Rev. E **69**, 036407 (2004).